

The Effect of Reinnervation on Force Production and Power Output in Skeletal Muscle¹

Kotaro Yoshimura, M.D.,* Hiroataka Asato, M.D.,* Paul S. Cederna, M.D.,†^{2,3}
Melanie G. Urbanek, Ph.D.,† William M. Kuzon, Jr., M.D., Ph.D.†⁴

*The Department of Plastic and Reconstructive Surgery, University of Tokyo, Tokyo, Japan; and †The Department of Surgery and The Institute of Gerontology, University of Michigan, Ann Arbor, Michigan 48109

Submitted for publication May 20, 1998

Failure to fully restore contractile function after denervation and reinnervation of skeletal muscle engenders significant disability in patients suffering peripheral nerve injuries. This work tested the hypothesis that skeletal muscle denervation and reinnervation result in a deficit in normalized power (W/kg), which exceeds the deficit in specific force (N/cm²), and that the mechanisms responsible for these deficits are independent. Adult Lewis rats underwent either transection and epineurial repair of the left peroneal nerve (denervation-reinnervation, $n = 13$) or SHAM exposure of the peroneal nerve (SHAM, $n = 13$). After a 4-month recovery period, isometric force, peak power, and maximum sustained power output were measured in the left extensor digitorum longus (EDL) muscle from each animal. Isometric force measurements revealed a specific force deficit of 14.3% in the reinnervated muscles. Power measurements during isovelocity shortening contractions demonstrated a normalized peak power deficit of 25.8% in the reinnervated muscles, which is accounted for by decreases in both optimal velocity (10.5%) and average force during shortening (13.7%). Maximum sustained power was similar in both groups. These data support our working hypothesis that both whole muscle force production and power output can be impaired in reinnervated muscle and that the relative deficits in power

output exceed the deficits in force production. The mechanisms responsible for the deficits in force production appear to be independent of those that result in changes in peak power output. The measurement of muscle power output may represent a clinically relevant variable for studies of the recovery of mechanical function after motor nerve injury and repair. © 1999

Academic Press

Key Words: reinnervated muscle; force production; power output.

INTRODUCTION

A primary obstacle to the effective rehabilitation of patients following peripheral motor nerve transection and repair is residual weakness in the involved skeletal muscles [1]. Despite significant advances in microsurgical nerve coaptation techniques, permanent disability occurs after virtually all immediate or delayed nerve reconstructions. These clinical observations are consistent with multiple experimental reports documenting residual force deficits in reinnervated skeletal muscle [2-6]. Muscle atrophy can account for the observed decrease in mean whole muscle isometric tetanic force (F_0), but an unexplained specific force deficit persists after force is normalized to total muscle cross-sectional area [3, 4, 6, 7]. Although it is possible to design interventions to counteract muscle atrophy, prevention of specific force deficits will not be possible until the responsible mechanisms are identified.

To date, research efforts in this area have focused primarily on measurements of isometric force, which is correlated primarily with the physiologic CSA of the muscle [8-12]. Power production, on the other hand, is dependent on muscle fiber-type composition, fiber length, cross-sectional area (CSA), force production

¹ This work was supported by a Grant from the Veterans Administration Merit Review Board.

² Dr. Cederna was supported by a grant from the National Institute on Aging, Multidisciplinary Research Training in Aging, Grant T32 AG00114.

³ To whom correspondence should be addressed at University of Michigan Medical Center, 2130 Taubman Center, 1500 East Medical Center Drive, Ann Arbor, MI 48109-0340. Fax: (734) 936-9657. E-mail: cederna@umich.edu.

⁴ Dr. Kuzon received support as the Academic Scholar of The American Association of Plastic Surgeons.

during shortening, and velocity of shortening. As such, measurements of peak and sustained power output following peripheral nerve injury and repair may be a more clinically relevant assessment of muscle mechanical function than isometric force production alone.

Using an animal model to simulate the clinical situation of a peripheral nerve injury and repair, this experiment was designed to measure changes in whole muscle force and power production after denervation and reinnervation. Our working hypotheses were as follows: (1) a specific force deficit will be identified after a skeletal muscle is denervated and reinnervated; (2) a deficit in peak power output during a single contraction will also be identified; (3) the power deficit will result from changes in both force production and velocity of shortening; and (4) the resultant normalized power deficit will exceed the specific force deficit.

MATERIALS AND METHODS

Preliminary Experiments

Although a comprehensive architectural analysis of limb muscles has been reported for several species of mammals [13–19], comparable data for Lewis rats have not been published. Therefore a preliminary investigation of the Lewis rat extensor digitorum longus (EDL) muscle fiber length and architecture was performed. To determine muscle fiber length (L_f), six 8-month-old male Lewis rats with body masses ranging from 400 to 500 g were utilized (Charles River Laboratories, Wilmington, MA). The length of the belly of the EDL muscle (L_m) was measured *in vivo* using a digital caliper. Muscles were harvested, secured at L_m , fixed in a 10% formaldehyde solution for 72 h, digested in 20% nitric acid for 4–5 days, and preserved in 50% glycerin solution [20, 21]. Individual muscle fibers were then dissected out of each muscle using microsurgical techniques (Zeiss OpMi-6, Carl Zeiss Inc., West Germany). The length of dissected fibers was measured using calipers and an average fiber length (L_f) was computed for each muscle. Based upon 360 fibers from 12 EDL muscles, the average L_f/L_m ratio for EDL muscles of adult Lewis rats was 0.35 ± 0.03 . Analysis of muscle architecture revealed a pinnation angle of less than 3° , which is consistent with the previously reported values for the same muscles in mice [11].

Animal Model

Experiments were performed using 4-month-old, male, specific pathogen-free Lewis rats with body masses ranging from 400 to 500 g. All animal care, housing, and operative procedures were conducted in accordance with the *United States Public Health Service Guide for the Care of Laboratory Animals* (NIH Publication Number 85-23); the experimental protocol was approved by the University Committee on the Use and Care of Animals. Rats were individually housed in a restricted access, pathogen-free facility in the Unit for Laboratory Medicine at the University of Michigan. Rats were provided food and water *ad libitum*, and were exposed to a 12 h light-dark cycle. For all surgical procedures, rats were anesthetized with an initial intraperitoneal injection of pentobarbital sodium (60 mg/kg); supplementary doses were administered to maintain a deep plane of general anesthesia. Surgical procedures were conducted under aseptic conditions.

Experimental Design and Paradigm

An experimental design was employed with surgical intervention (sham surgery vs denervation-reinnervation) as the main effect,

independent variable. Animals were allocated to one of two groups with the restriction that equal numbers would be assigned to each group. The groups studied were (1) division and immediate repair of the left peroneal nerve to the EDL muscle (denervation-reinnervation group) and (2) sham exposure of the peroneal nerve (SHAM group). In animals undergoing denervation-reinnervation procedures, the peroneal nerve to the EDL muscle was isolated through a short left lateral thigh incision. The peroneal nerve was sharply divided 2–4 mm from the EDL muscle and immediately repaired under an operating microscope with an epineurial technique, using interrupted sutures of 10-0 nylon. The wound was then closed in layers with interrupted simple sutures of 4-0 chromic. Great care was taken not to injure any EDL muscle fibers during the operative procedure. In animals undergoing sham procedures, an identical peroneal nerve isolation procedure was performed, except the nerve was not divided or sutured. After the initial surgical procedure, animals were allowed to recover in standard cages for 4 months before a second operative procedure was performed to measure EDL contractile properties.

Measurement of Muscle Contractile Properties

In situ measurements of force production and power output were made in the EDL muscle 4 months after the initial surgery in a manner similar to that previously described [22, 23]. Each rat was anesthetized and the left EDL was isolated without injuring the neurovascular pedicle. The distal tendons of the EDL were identified over the dorsum of the foot, divided, and folded to create a tendon loop. The loop was secured at the musculotendinous junction with 4-0 silk sutures, and later used to affix the distal tendons to the servomotor lever arm. To avoid motion artifact from adjacent muscle groups during the *in situ* measurements, the peroneus, gastrocnemius, soleus, plantaris, and tibialis anterior muscles were divided and reflected. The sciatic nerve was identified and exposed throughout its course in the lateral thigh. The tibial and sural branches were divided above the level of the knee. The branches of the peroneal nerve to the EDL were preserved, all other branches were divided. The rat was placed on a platform maintained at 35°C with a temperature-controlled water circulator. To stabilize the left leg during force and power measurements, the femoral condyle and foot were secured to the platform. The EDL tendon loop was secured to the lever arm of a servomotor (Cambridge Technology Inc., Model 300H, Cambridge, MA). Throughout the evaluation, the EDL muscle and peroneal nerve were regularly bathed with warm mineral oil (36°C); muscle temperature was monitored and maintained between 35 and 36°C .

Force measurements. The EDL muscles were activated indirectly with supramaximal nerve stimuli (square pulses, 0.2-ms pulse duration, 2–6 V) generated by a Grass S88 stimulator (Grass Instrument Co., Quincy, MA) and delivered to the peroneal nerve, proximal to the nerve coaptation site, using a shielded bipolar silver wire electrode (Harvard Apparatus, South Natick, MA). Force output at the muscle tendon was transduced using the servomotor and displayed on a storage oscilloscope (Gould Inc., Romulus, MI). The position of the servomotor lever arm was controlled with a microcomputer (Dell Computer Corp., Austin, TX) equipped with a digital to analogue converter (Data Translation, Marlboro, MA) and custom software (Asyst Software Technologies, Inc., Rochester, NY). The microcomputer also sampled force data during contractions via analogue to digital channels on the Data Translation board. Twitch contractions were used to determine the optimal length for force production (L_o). With the muscle set at this length, a single 300-ms stimulation at 80 Hz was delivered, and L_o was again checked using twitch contractions. All subsequent isometric force measurements were made at L_o . Using calipers, L_o was then measured directly as the total length of the muscle, excluding the tendons of origin and insertion. During single twitch contractions, peak twitch force (F_T) was measured. To measure maximum isometric tetanic force (F_o), the EDL muscle was stimulated for 250 ms at increasing frequencies

from 30 to 350 Hz. Two minutes elapsed between tetanic contractions to permit muscle recovery. The force plateau was defined as F_o . The total muscle fiber CSA ("physiologic CSA") was then determined according to the following [24, 25].

$$CSA = \frac{m_{mass} \cdot \cos \theta}{(\rho)(L_o)(0.35)}, \quad (1)$$

where CSA = muscle fiber cross-sectional area, m_{mass} = muscle mass, θ = angle of pinnation, ρ = density of mammalian skeletal muscle (1.06 g/cm³), L_o = optimal muscle length for force production, and 0.35 = L_f/L_m ratio determined from preliminary experiments.

The maximum specific isometric tetanic force (sF_o) was calculated as the maximum tetanic force (F_o) normalized to muscle physiologic CSA.

Peak power measurements. All measurements of peak power were made as described by Brooks *et al.* [23, 26]. Force and power were measured during isovelocity shortening contractions. To permit muscle shortening as close to L_o as possible, the lever arm of the servomotor was programmed to displace the muscle through 12% of L_f . The muscles were prestretched to 106% of L_f and then shortened to 94% of L_f . The peroneal nerve was stimulated simultaneously with the initiation of the shortening ramp and throughout the duration of the shortening ramp. The average force (F_c) generated during a single shortening contraction was determined by calculating the area under the force curve. The power during a single contraction was calculated as the product of F_c and the velocity of shortening. The velocity of shortening was increased incrementally until the maximum power (P_{max}) was achieved and further increases in velocity resulted in lower power. The velocity at which maximum power occurred was termed V_{opt} , the optimal shortening velocity for the generation of power. V_{opt} was determined for a range of stimulation frequencies up to 500 HZ. The power during a single contraction was plotted against the stimulation frequency to construct a power-frequency curve; peak power (P_{max}) was defined as the maximum power measured at V_{opt} . The normalized peak power (nP_{max}) was then calculated by dividing the P_{max} by muscle mass.

Sustained power measurements. The sustained force (F_s) and sustained power (P_s) were then evaluated using a series of isovelocity shortening contractions with increasing duty cycles (C_d). The duty cycle is the fraction of time during the work-rest cycle when work is performed by the muscle. The stimulation frequency which produced approximately 85% F_o was used while determining F_s and P_s (range 120–150 Hz). The velocity of shortening (L_f/s) selected for determining P_s was the velocity which produced the maximum power at the previously defined stimulation frequency. The time of each contraction was constant, but the train rate was increased, thus increasing C_d . An initial duty cycle of 0.01 was utilized. The muscles were stimulated at the initial duty cycle for approximately 1 min before a steady-state force was generated. The muscles were then stimulated for an additional 5 min before gradually increasing the C_d . The final contraction of each stimulation interval was then used for the calculation of sustained power. The sustained power was calculated as follows:

$$P_s = (F_c)(C_d)(V_{opt}). \quad (2)$$

C_d was then increased, and the entire process was repeated. The duty cycle was increased until the maximal sustained power was determined. The normalized maximal sustained power (nP_s) was then calculated by dividing the maximum sustained power by muscle mass.

F_s was then calculated as the product of F_c and C_d . The average force generated during the last contractions of the 5-min stimulation periods was used for calculation of F_s .

After completion of the force and power measurements, the EDL was then harvested from the animal, the tendons were trimmed, and

the muscle was weighed. All muscles were covered with cryopreservative, frozen with isopentane cooled by liquid nitrogen (160°C), and stored at -60°C for subsequent histochemical processing. The animal was euthanized with a lethal injection of pentobarbital sodium.

Histochemical Analysis

Fiber-type determination. Serial, transverse, 10- μ m-thick cross sections were obtained in a cryostat from the middle third of the EDL muscle. The tissues were stained with hematoxylin and eosin (H&E), succinate dehydrogenase (SDH) [27], and myosin ATPase (mATPase) at five different pH's (10.4, 9.4, 4.5, 4.3, and 3.8) [28–31]. Muscle fibers were classified as either slow oxidative (SO), fast oxidative glycolytic (FOG), or fast glycolytic (FG), based upon differential staining to mATPase and SDH [18, 32]. In each muscle, the percentage of SO, FOG, and FG fibers in the whole muscle cross sections was determined by a direct count of all fibers in the cross section using established techniques [33].

Fiber-type area fraction measurements. The CSA of all EDL muscles and all individual muscle fibers was determined using computerized planimetry (Bioquant, R and M Biometrics, Inc., Nashville, TN) in accordance with previously established methods [29, 32]. From the muscle fiber-type distribution and fiber CSA data, the relative CSA fraction for Types SO, FOG, and FG fibers was computed [34].

$$\text{Relative Area Type SO} = \frac{(\% \text{ SO})(\text{Area SO})}{(\% \text{ SO})(\text{Area SO}) + (\% \text{ FOG}) \times (\text{Area FOG}) + (\% \text{ FG})(\text{Area FG})}, \quad (3)$$

where % SO = SO fiber percentage, % FOG = FOG fiber percentage, % FG = FG fiber percentage, Area SO = mean CSA for SO fibers, Area FOG = mean CSA for FOG fibers, and Area FG = mean CSA for FG fibers.

Data Analysis

The mean and standard deviation of each variable measured were computed for each group. For measurements of muscle mass, body mass, and each variable related to muscle contractile properties, the significance of the main effect of surgical intervention (SHAM vs denervation-reinnervation) was determined using the unpaired Student's *t* test. Differences in muscle fiber-type composition between groups were evaluated using χ^2 analysis with muscle fiber type (SO, FOG, or FG) and surgical intervention (SHAM vs denervation-reinnervation) as the row and column variables, respectively. Significant differences in the relative CSA occupied by each fiber type were sought using two-way analysis of variance (ANOVA). *Post hoc* comparison of individual group means was performed only if the *F* ratio for the overall ANOVA was significant; appropriate Bonferroni corrections were applied to all *post hoc* comparisons. Statistical computations were performed using a microcomputer and the Statistical Analysis System (SAS, Inc., Cary, NC). For this study, α was set at 0.05.

RESULTS

Twenty-six animals were entered into the study ($n = 13$ for each group). One animal from the SHAM group failed to complete the protocol leaving data from 25 animals for analysis. The rats tolerated the initial surgical procedure well and demonstrated no long-term gait or behavioral abnormalities. The SHAM and denervation-reinnervation groups were not significantly different in relation to body mass, muscle mass, L_o , or CSA (Table 1).

TABLE 1

Isometric Force Measurements: SHAM versus Denervated-Reinnervated EDL Muscles

	SHAM (n = 12)	Denervated-reinnervated (n = 13)
Body mass (g)	456.8 ± 21.8	464.8 ± 15.3
Muscle mass (g)	195.3 ± 12.7	195.4 ± 17.6
L_f (mm)	14.8 ± 0.51	14.5 ± 0.40
CSA (mm ²)	12.5 ± 0.70	12.8 ± 1.17
F_i (mN)	711.9 ± 90.1	583.0 ± 129.0*
F_o (mN)	4082.2 ± 321.4	3585.8 ± 549.2*
sF_o (kN/m ²)	327.7 ± 21.4	280.7 ± 33.0*

Note. Data are displayed as means ± standard deviation of mean. Muscle mass, given in wet muscle mass; L_f , muscle fiber length; CSA, cross-sectional area of EDL muscle; F_i , maximum isometric twitch force; F_o , maximum isometric tetanic force; sF_o , maximum specific tetanic force.

* Statistically significant at $P < 0.05$, denervated-reinnervated vs SHAM.

Force Measurements

Isometric force measurements are summarized in Table 1. The maximum isometric twitch (F_i) and tetanic (F_o) forces were significantly lower in the reinnervated muscles compared to SHAM muscles. When F_o was normalized to the muscle physiologic CSA, a statistically significant specific force deficit was identified in the reinnervated, compared with SHAM, EDL muscles (280.7 ± 33.0 versus 327.7 ± 21.4 kN/m²).

Maximum Power Measurements

All power measurements are summarized in Table 2. Peak power during a single isovelocity shortening contraction increased as the stimulation frequency was increased from 100 to approximately 350 Hz. A subsequent decrease in power was realized as the frequency was increased beyond 350 Hz. The power-frequency curves for the two groups were parallel. P_{max} and nP_{max} deficits of 24.5 and 25.8%, respectively, were identified in the reinnervated muscles; these deficits are substantially greater than the previously identified sF_o deficit of 14.4%. The demonstrated power deficits were associated with decreases in both optimal velocity of shortening for the development of power (10.5% decrease) and average force during shortening (13.7% decrease). The P_{max} deficit is completely accounted for by these two variables.

Sustained Power Measurements

There was no statistically significant difference between SHAM and denervated-reinnervated muscles in relation to maximum or normalized sustained power during isovelocity shortening contractions. Additionally, the effect of duty cycle (work/rest ratio) on P_s and nP_s was similar in the two groups.

TABLE 2

Power Measurements: SHAM versus Denervated-Reinnervated EDL Muscles

	SHAM (n = 12)	Denervated-reinnervated (n = 13)
V_{opt} (L_f/s)	2.00 ± 0.11	1.79 ± 0.24*
P_{max} (mW)	41.50 ± 4.51	31.42 ± 6.24*
nP_{max} (W/kg)	213.14 ± 22.73	158.12 ± 31.43*
F_s (N)	1.402 ± 0.15	1.21 ± 0.24*
C_d	0.097 ± 0.061	0.11 ± 0.063
P_s (mW)	0.697 ± 0.14	0.949 ± 0.38
nP_s (W/kg)	3.55 ± 0.73	4.75 ± 1.95

Note. Data are displayed as means ± standard deviation of mean. V_{opt} , optimum velocity for maximum power; P_{max} , maximum power during isovelocity shortening contractions; through 10% of L_f , at optimum velocity; nP_{max} , normalized power = maximum power/muscle wet mass; F_s , sustained force = average force during shortening × duty cycle; C_d , duty cycle (ratio of work/rest); P_s , maximum power sustained during repeated isovelocity shortening contractions; nP_s , normalized sustained power = $sPow$ /muscle wet mass.

* Statistically significant at $P < 0.05$, denervated-reinnervated vs SHAM.

EDL Histomorphometry

A significant change in muscle fiber-type composition was identified in EDL muscles from animals in the denervation-reinnervation group (Table 3). SO fibers accounted for 3.9% of the total EDL muscle fibers in the SHAM animals, and 11.9% in the reinnervated animals ($P < 0.001$). When compared with controls, the percentages of FOG and FG fibers in reinnervated EDL muscles were reduced by 4.0 and 4.1%, respectively. Type grouping and occasional atrophic fibers were observed in the reinnervated muscles (Fig. 1). However, despite these significant changes in fiber-type percentages, the relative

TABLE 3

Histomorphometry of SHAM versus Denervated-Reinnervated EDL Muscle

Variable	Fiber type	SHAM (n = 9)	Denervated-reinnervated (n = 12)
Muscle fibers (%)	SO	3.9 ± 0.8	11.9 ± 3.6*
	FOG	35.4 ± 5.5	31.4 ± 8.1
	FG	60.7 ± 5.9	56.6 ± 9.7
CSA (%)	SO	1.3 ± 0.4	3.8 ± 1.2
	FOG	30.5 ± 7.5	31.8 ± 14.2
	FG	68.2 ± 7.6	64.4 ± 15.0

Note. Data are displayed as means ± standard deviation of mean. Muscle fibers (%), relative number fraction of each fiber type, per muscle; CSA (%), relative area fraction of each fiber type; SO, slow oxidative muscle fiber; FOG, fast oxidative glycolytic; FG, fast glycolytic.

* Statistically significant at $P < 0.001$, SHAM vs denervated-reinnervated.

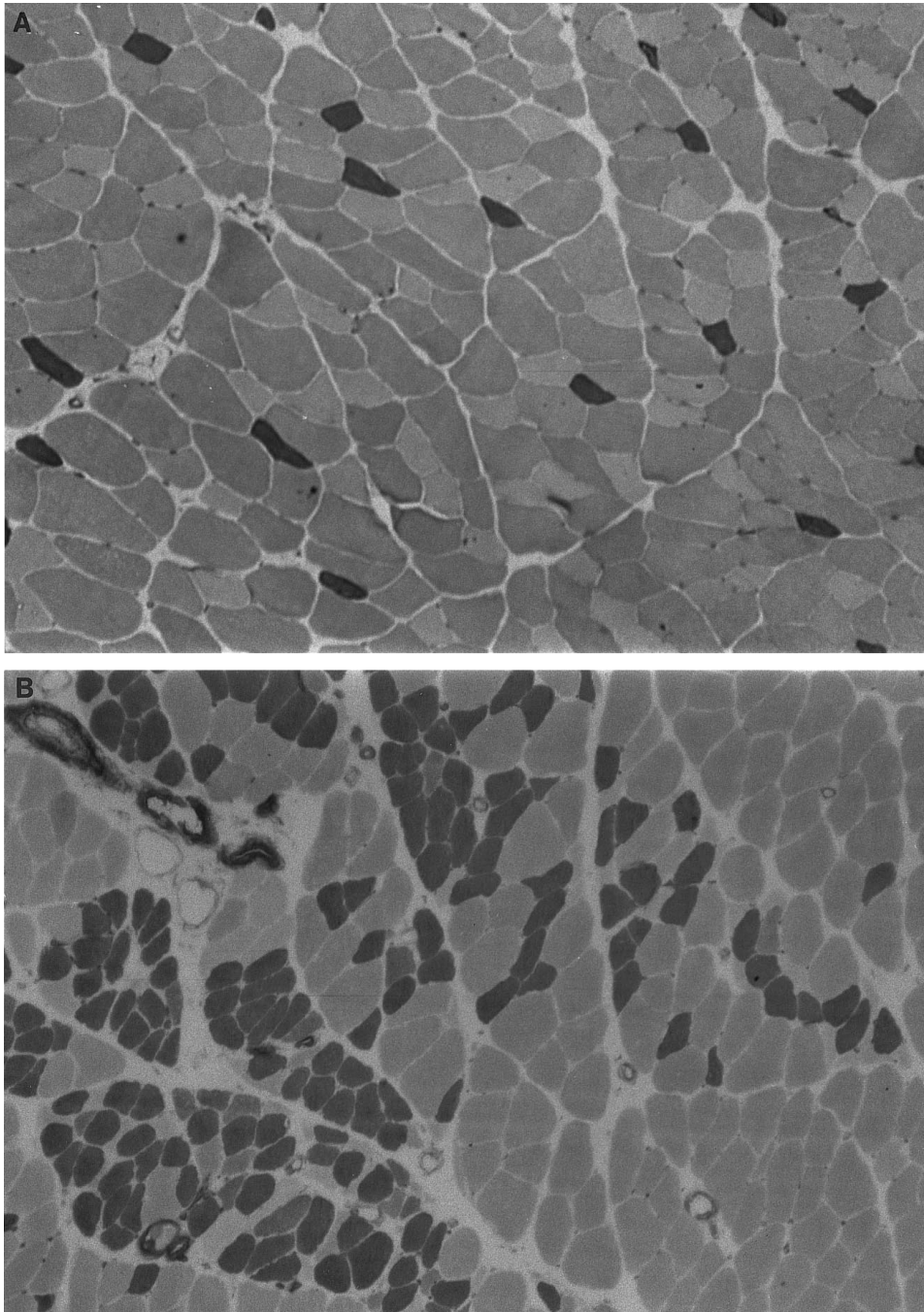


FIG. 1. Low-power (15 \times) photomicrograph of extensor digitorum longus muscles stained for myosin-ATPase (pH 4.5). Slow fibers stain darkly, fast fibers stain lightly. (A) SHAM muscle demonstrating normal fiber-type composition and spatial organization. (B) Denervated and reinnervated muscle demonstrating an increased percentage of slow fibers and fiber-type grouping.

CSA occupied by each fiber type did not change after denervation and reinnervation of the EDL muscle.

DISCUSSION

These data support our four working hypotheses. First, a significant specific force deficit exists in skeletal muscle reinnervated under the conditions of this

experiment. Muscle atrophy can partially account for the observed decrease in reinnervated whole muscle mean isometric tetanic force, but cannot account for the specific force deficit identified. An additional mechanism must be contributing to this force deficit. Second, a deficit in peak power output during a single contraction is identified in reinnervated muscle. Third, this power deficit is the result of reductions in both

force production and optimum velocity of shortening. Fourth, a 25.8% deficit in mean normalized peak power was identified in the reinnervated EDL muscle of the rat, exceeding the mean specific force deficit of 14.4% in the same muscle by nearly twofold. The cumulative effect of a 10.5% reduction in optimal velocity and a 13.7% decrease in force production during shortening was responsible for this normalized peak power deficit.

Type grouping and a greater percentage of SO fibers was observed in the reinnervated compared with control EDL muscles. Both of these observations have been made repeatedly for reinnervated skeletal muscle [35–43]. Although abundant experimental evidence supports a relationship between muscle fiber-type composition and rates of force development and shortening [44–48], it is unlikely that fiber-type composition or spatial organization changes contributed to the observed changes in the contractile properties of EDL muscles from animals in the denervation-reinnervation group for two reasons. First, although there was an increase in the number of SO fibers in reinnervated muscle, there was no appreciable change in the relative CSA occupied by SO, FOG, and FG fibers, due to the comparatively small CSA of the SO fibers relative to FOG and FG fibers. Because the relative CSA occupied by each fiber type did not change, it is unlikely that changes in fiber-type composition contributed to the large observed changes in muscle contractile properties. Second, there is no experimental evidence indicating that type grouping alone can result in whole muscle force or peak power deficits. Mechanisms besides changes in fiber-type composition must contribute to the force and power deficits observed in the reinnervated EDL muscles.

We chose to measure the optimum velocity of shortening and peak power output for several reasons. In muscles with heterogeneous fiber types, measurements of V_{\max} along the steep portion of the force-velocity curve are more reflective of FOG and FG muscle fiber function, rather than whole muscle function [49]. In addition, at lower loads, the slope of the force-velocity curve is so steep that minor errors in measurements will result in widely divergent V_{\max} measurements [50]. Activities such as jumping, sprinting, heavy lifting, and many other whole organism movements require optimization of power, rather than force development, so that determining the optimal velocity for the development of maximum power, rather than the maximal velocity of shortening, permits reliable measurement of a parameter with distinct physiological meaning [51]. In our experiment, the reinnervated muscles developed significantly lower maximum power and normalized maximum power when compared with control muscles. The 24.3% maximum power deficit observed in reinnervated muscles as compared to the SHAM muscles resulted from a 10.5% reduction in the

optimal velocity and a 13.7% reduction in force. Note that our observed decrease in optimum velocity for power generation occurred without a significant shift in fiber-type CSA; this has been previously observed in experiments concerning physical conditioning or deconditioning [52–54]. After reinnervation, therefore, the reduction in power output is due to mechanisms influencing the velocity of shortening in addition to those affecting force generation. This is underscored by our observation that, in the reinnervated EDL muscles, the 26% deficit in normalized peak power production is nearly twofold greater than the 14% specific force deficit. These findings may be significant because the recovery of power production may be the most clinically relevant factor in the rehabilitation of patients after nerve injury.

We observed no significant difference in the absolute and normalized sustained power output between the SHAM and reinnervated groups. It has been hypothesized that differences in the capacity to sustain power is due to differences in the types of muscle fibers present [55]. In this experimental model of denervation and reinnervation, no significant shifts in fiber type CSA were identified. Therefore, no substantial change in sustained power output was expected following the reinnervation of rat EDL muscles. This finding underscores the concept that, following reinnervation, mechanisms responsible for deficits in whole muscle force production, in peak power development during a single contraction, or in sustained power capacity may be disparate and may operate independently, depending on the precise experimental circumstances.

Patients who sustain a peripheral nerve injury and repair frequently complain of muscle weakness and diminished endurance. The observed decreases in sF_0 and nP_{\max} are consistent with clinical complaints of weakness after nerve injury. On the other hand, the clinical complaint of easy fatigability is seemingly inconsistent with our finding that sustained power output was unchanged in the reinnervated rat EDL muscles. However, fatigue is defined as a reduction in force, not in power production [56]. Although the EDL muscles from the denervated-reinnervated group were able to sustain power output at the same level as control muscles, they did so mainly by maintaining a higher duty cycle, and, in fact, the mean force produced during the sustained power protocol was significantly lower in the denervated-reinnervated EDL muscles than in controls (Table 1). This diminished force during sustained contractions may be perceived clinically as fatigue, even though overall power output is unchanged. Obviously, further work will be required to delineate changes in force production and power output under a variety of clinical and experimental circumstances.

The experimental model was selected to specifically address the effect of skeletal muscle denervation and

reinnervation on force production and power output under circumstances where an optimum recovery could be anticipated. The peroneal nerve was sharply divided a very short distance from the neuromuscular junctions and immediately repaired, providing optimal conditions for axonal regeneration and neuromuscular synaptogenesis. The proximity of the neuroorrhaphy to the EDL muscle (2–4 mm) maximizes the potential for rapid reinnervation and minimizes the functional sequelae of prolonged muscle denervation, including atrophy and fibrosis. In addition, a direct epineural neuroorrhaphy provides the opportunity for axonal regeneration within the endoneural conduits in the distal nerve stump. Previous studies have demonstrated that this route for axonal regeneration is far more efficient in promoting muscle fiber reinnervation than neurotization with axons regenerating outside the basal lamina conduits [57–59]. Although we cannot exclude the possibility that some autoreinnervation of the denervated EDL muscle occurred exclusive of the neuroorrhaphy, it seems unlikely that such reinnervation would confound our results by substantially contributing to the functional recovery of the reinnervated muscle.

Therefore, the force and power deficits in the reinnervated rat EDL muscles in our study were observed even under experimental conditions optimized for maximum recovery. Clinically, a peripheral nerve injury and repair rarely occur under these optimal conditions. In the clinical setting, prolonged atrophy, fibrosis, and other mechanisms likely contribute to more substantial deficits in muscle contractile function than those observed here.

CONCLUSIONS

Denervation and reinnervation are deleterious to the mechanical function of skeletal muscle. Using the rat EDL muscle as a model of muscle denervation and reinnervation, we have demonstrated that both whole muscle force production and power output are impaired in reinnervated muscle and that the mechanisms responsible for deficits in force production appear to be independent of those that result in changes in peak or sustained power output. In reinnervated muscle, relative deficits in power output may exceed those in force production, and power measurements may represent a more clinically relevant variable for studies of the recovery of muscle mechanical function after motor nerve injury and repair. Further research should be directed at determining the mechanisms responsible for force and power deficits in reinnervated skeletal muscle.

REFERENCES

- MacKinnon, S. *Surgery of the Peripheral Nerve*. New York: Theime Medical Publishers, 1988.
- MacKinnon, S., Dellon, A. L., Hudson, A. R., and Hunter, D. A. Nerve regeneration through a pseudosynovial sheath in a primate model. *Plast. Reconstr. Surg.* **75**: 833, 1985.
- Cheng, N., Li, X., and Huang, A. Experimental comparison of muscle contractility after three methods of reinnervation. *Ann. Plast. Surg.* **33**: 166, 1994.
- Hems, T., and Glasby, M. Comparison of different methods of repair of long peripheral nerve defects: An experimental study. *Br. J. Plast. Surg.* **45**: 497, 1992.
- Kuypers, P. D. L., vanEgeraat, J. M., Godschalk, M., and Hovius, S. E. R. Loss of viable neuronal units in the proximal stump as possible cause for poor functional recovery following nerve reconstructions. *Exp. Neurol.* **132**: 77, 1995.
- Kuzon, W. M., Asato, H., and Youssef, M. Force deficit after skeletal muscle reinnervation. *Surg. Forum* **45**: 630, 1994.
- Asato, H., and Kuzon, W. M. Muscle contractile function after repeated denervation and reinnervation. In M. Frey and P. Giovanoli (Eds.), *Proc. 4th International Muscle Symposium, Zurich, 1995*. Pp. 82–84.
- Terzis, J. K., Sweet, R. C., Dykes, R. W., and Williams, H. B. Recovery of function in free muscle transplants using microneurovascular anastomosis. *J. Hand Surg.* **3**: 37, 1978.
- Frey, M., Gruber, H., Havel, M., Steiner, E., and Freilinger, G. Experimental free muscle transplantation with microneurovascular anastomosis. *Plast. Reconstr. Surg.* **71**: 689, 1983.
- Guelinckx, P., Faulkner, J., and Essig, D. Neurovascular anastomosed muscle grafts in rabbits: Functional deficits result from tendon repair. *Muscle Nerve* **11**: 745, 1988.
- Lewis, D. M., Parry, D. J., and Rowleron, A. Isometric contractions of motor units and immunohistochemistry of mouse soleus muscle. *J. Physiol. Lond.* **325**: 393, 1982.
- Guelinckx, P., Faulkner, J. A., and Essig, D. Rectus femoris muscles of rabbits autografted with microvascular repair with nerves intact or nerves anastomosed. In M. Frey and G. Freilinger, (Eds.), *2nd Vienna Muscle Symposium, Proceedings*. Austria, Facultas Universitätsverlag. Pp. 75–83, 1976.
- Burkholder, T. J., Fingado, B., Baron, S., and Lieber, R. L. Relationship between muscle fiber types and sizes and muscle architectural properties in the mouse hindlimb. *J. Morphol.* **221**(2): 177, 1994.
- Friederich, J. A., and Brand, R. A. Muscle fiber architecture in the human lower limb. *J. Biomech.* **23**(1): 91, 1990.
- Jacobson, M. D., Raab, R., Fazeli, B. M., Abrams, R. A., Botte, M. J., and Lieber, R. L. Architectural design of the human intrinsic hand muscles. *J. Hand Surg. Am. Vol.* **17**(5): 804, 1992.
- Lieber, R. L., and Blevins, F. T. Skeletal muscle architecture of the rabbit hindlimb: Functional implications of muscle design. *J. Morphol.* **199**(1): 93, 1989.
- Lieber, R. L., Jacobson, M. D., Fazeli, B. M., Abrams, R. A., and Botte, M. J. Architecture of selected muscles of the arm and forearm: Anatomy and implications for tendon transfer [see comments]. *J. Hand Surg. Am. Vol.* **17**(5): 787, 1992.
- Sacks, R. D., and Roy, R. R. Architecture of the hind limb muscles of cats: Functional significance. *J. Morphol.* **173**(2): 185, 1982.
- Wickiewicz, T. L., Roy, R. R., Powell, P. L., and Edgerton, V. R. Muscle architecture of the human lower limb. *Clin. Orthop.* **179**: 275, 1983.
- Maxwell, L. C., Faulkner, J. A., Mufti, S. A., and Turowski, A. M. Free autografting of entire limb muscles in the cat: Histochemistry and biochemistry. *J. Appl. Physiol.* **44**: 431, 1978.
- Segal, S. S., and Faulkner, J. A. Temperature dependent phys-

- iological stability of rat skeletal muscle in vitro. *Am. J. Physiol.* **258**: C265, 1985.
22. Brooks, S. V., Faulkner, J. A., and McCubrey, D. A. Power outputs of slow and fast skeletal muscles of mice. *J. Appl. Physiol.* **68**: 1282, 1990.
 23. Brooks, S. V., and Faulkner, J. A. Maximum and sustained power of extensor digitorum longus muscles from young, adult, and old mice. *J. Gerontol.* **46**: 28, 1991.
 24. Mendez, J., and Keys, A. Density and composition of mammalian muscle. *Metabolism* **9**: 1984, 1960.
 25. Gans, C. Fiber architecture and muscle function. *Exer. Sport Sci. Rev.* **10**: 160, 1982.
 26. Brooks, S. V., and Faulkner, J. A. Forces and power of slow and fast skeletal muscles in mice during repeated contractions. *J. Physiol.* **436**: 701, 1991.
 27. Nachlas, M. M., Tsou, K., DeSouza, E., Cheng, C., and Seligman, A. M. Cytochemical demonstration of succinic dehydrogenase by the use of a new *p*-nitrophenyl substituted ditetrazole. *J. Histochem. Cytochem.* **5**: 420, 1957.
 28. Rosenblatt, J., Kuzon, W. M., Plyley, M., Pynn, B., and McKee, N. A histochemical method for the simultaneous demonstration of capillaries and fibers in skeletal muscle. *Stain Technol.* **62**: 263, 1988.
 29. Kuzon, W. M., Rosenblatt, J., Pynn, B., Plyley, M., and McKee, N. Fiber type morphometry and capillary geometry in free, vascularized muscle transfers. *Microsurgery* **12**: 352, 1991.
 30. Brooke, M. H. Muscle fiber types: How many and what kind. *Arch. Neurol.* **23**: 369, 1970.
 31. Blomstrand, E., Celsing, F., Friden, J., and Ekblom, B. How to calculate human muscle fibre areas in biopsy samples-methodologic considerations. *Acta Physiol. Scand.* **122**: 545, 1984.
 32. Blomstrand, E., and Ekblom, B. The needle biopsy technique for fibre type determination in human skeletal muscle—a methodological study. *Acta Physiol. Scand.* **116**: 437, 1982.
 33. Green, H., Reichmann, H., and Pette, D. A comparison of two ATPase based schemes for histochemical muscle fibre typing in various mammals. *Histochemistry* **76**: 21, 1982.
 34. Halkjaer-Kristensen, J., and Ingemann-Hansen, T. Wasting of the human quadriceps muscle after knee ligament injuries. *Scand. J. Rehabil. Med. Suppl.* **13**: 5, 1985.
 35. Foehring, R. C., Syper, G. W., and Munson, J. B. Properties of self-reinnervated motor units of medial gastrocnemius of cat. I. Long-term reinnervation. *J. Neurophysiol.* **55**: 931, 1986.
 36. Das, S., Spector, S., Miller, T., Martin, T., and Edgerton, V. Model for microvascular muscle transplantation in the dog. *Plast. Reconstr. Surg.* **77**: 804, 1986.
 37. Stenanovic, M. V., Seaber, A. V., and Urbaniak, J. R. Canine experimental free muscle transplantation. *Microsurgery* **7**: 105, 1986.
 38. Karpati, G., and Engel, W. Type grouping in skeletal muscles after experimental reinnervation. *Neurology* **18**: 447, 1968.
 39. Gordon, T., and Stein, R. B. Reorganization of motor-unit properties in reinnervated muscles of the cat. *J. Neurophysiol.* **48**: 1175, 1982.
 40. Dubowitz, V. Cross-innervated mammalian skeletal muscle: Histochemical, physiological, and biochemical observations. *J. Physiol.* **193**: 481, 1967.
 41. Dettbarn, W. D. A distinct difference between slow and fast muscle in acetylcholinesterase recovery after reinnervation in the rat. *Exp. Neurol.* **74**: 33, 1981.
 42. Albani, M., Lowrie, M. B., and Vrbova, G. Reorganization of motor units in reinnervated muscles of the rat. *J. Neurol. Sci.* **88**: 195, 1988.
 43. Eisen, A., Karpati, G., Carpenter, S., and Danon, J. The motor unit profile of the rat soleus in experimental myopathy and reinnervation. *Neurology* **24**: 878, 1974.
 44. Howald, H. Training induced morphological and functional changes in skeletal muscle. *Int. J. Sports Med.* **3**: 1, 1982.
 45. Jolesz, F., and Sreter, F. Development, innervation, and activity pattern induced changes in skeletal muscle. *Annu. Rev. Physiol.* **43**: 531, 1981.
 46. Close, R. Dynamic properties of mammalian skeletal muscles. *Physiol. Rev.* **52**: 129, 1972.
 47. Close, R. Properties of motor units in fast and slow skeletal muscles of the rat. *J. Physiol. Lond.* **193**: 45, 1967.
 48. Barany, M. ATPase activity of myosin correlated with speed of muscle shortening. *J. Gen. Physiol.* **50**: 197, 1967.
 49. Claffin, D. R., and Faulkner, J. A. The force-velocity relationship at high shortening velocities in the soleus muscle of the rat. *J. Physiol. Lond.* **411**: 627, 1989.
 50. Podolin, R. A., and Ford, L. E. Influence of partial activation on force-velocity properties of frog skinned muscle fibers in millimolar magnesium ion. *J. Gen. Physiol.* **87**: 607, 1986.
 51. Jones, N. L., McCartney, N., and McComas, A. J. *Human Muscle Power*. Champaign, IL: Human Kinetics Pub., 1986.
 52. Bangart, J. J., Widrick, J. J., and Fitts, R. H. Effect of intermittent weight bearing on soleus fiber force-velocity-power and force-pCa relationships. *J. Appl. Physiol.* **82**(6): 1905, 1997.
 53. McDonald, K. S., Blaser, C. A., and Fitts, R. H. Force-velocity and power characteristics of rat soleus muscle fibers after hind-limb suspension. *J. Appl. Physiol.* **77**(4): 1609, 1994.
 54. Widrick, J. J., Bangart, J. J., Karhanek, M., and Fitts, R. H. Soleus fiber force and maximal shortening velocity after non-weight bearing with intermittent activity. *J. Appl. Physiol.* **80**(3): 981, 1996.
 55. Faulkner, J. A. Power output of the human diaphragm. *Am. Rev. Respir. Dis.* **134**: 1081, 1986.
 56. Segal, S. S., Faulkner, J. A., and White, T. P. Skeletal muscle fatigue in vitro is temperature dependent. *J. Appl. Physiol.* **61**: 660, 1986.
 57. Carlson, B. M., Billington, L., and Faulkner, J. A. Studies on the regenerative recovery of long-term denervated muscles in rats. *Restor. Neuro. Neurosci.* **10**: 77, 1996.
 58. Harrison, I. W., Speirs, V. C., Braund, K. G., and Steiss, J. E. Attempted reinnervation of the equine larynx using muscle pedicle graft. *Cornell Vet.* **82**: 59, 1992.
 59. Klueber, K. M. Role of muscle neurotization in the reinnervation of murine muscle grafts. *Anat. Rec.* **219**: 370, 1987.